



Investigation of therapeutic potential of cerium oxide nanoparticles in Alzheimer's disease using transgenic *Drosophila*

Vignesh Sundararajan¹ · G. Devanand Venkatasubbu² · Sahabudeen Sheik Mohideen¹

Received: 24 September 2020 / Accepted: 23 February 2021 / Published online: 6 March 2021
© King Abdulaziz City for Science and Technology 2021

Abstract

In the current study, the therapeutic potential of cerium oxide nanoparticles ($n\text{CeO}_2$) was investigated in a human tau (htau) model of Alzheimer's disease (AD), using *Drosophila melanogaster* as an in vivo model. $n\text{CeO}_2$ synthesised via the hydroxide-mediated approach were characterised using Fourier transform infrared (FTIR), transmission electron microscopy (TEM), X-ray diffraction (XRD) analyses and Raman spectroscopy. Characterisation studies confirmed the formation of pure cubic-structured $n\text{CeO}_2$ and showed that the particles were spherically shaped, with an average size between 20 and 25 nm. The synthesised $n\text{CeO}_2$ were then administered as part of the diet to transgenic *Drosophila* for one month, at 0.1 and 1 mM concentrations, and its effect on the biochemical levels of superoxide dismutase (SOD), acetylcholinesterase (AChE), and the climbing activity of flies were studied in a pan-neuronal model (elav; htau) of AD. Using an eye-specific model of htau expression (GMR; htau), the effect of $n\text{CeO}_2$ on htau and autophagy-related (ATG) gene expression was also studied. Dietary administration of $n\text{CeO}_2$ at a concentration of 1 mM restored the activity of SOD similar to that of control, but both concentrations of $n\text{CeO}_2$ failed to modulate the level of AChE, and did not elicit any significant improvements in the climbing activity of elav; htau flies. Moreover, $n\text{CeO}_2$ at a concentration of 1 mM significantly affected the climbing activity of elav; htau flies. $n\text{CeO}_2$ also elicited a significant decrease in htau gene expression at both concentrations and increased the mRNA expression of key autophagy genes ATG1 and ATG18. The results therefore indicate that $n\text{CeO}_2$ aids in replenishing the levels of SOD and tau clearance via the activation of autophagy.

Keywords Acetylcholinesterase · Autophagy · Human tau · Locomotor activity · Superoxide dismutase

Introduction

Alzheimer's disease (AD) is a disorder of the brain and nervous system which commonly causes dementia. The major symptoms of AD include decline in cognitive domains such as visuospatial functions memory, language and behaviour

which in turn greatly affect the ability of the patient to perform day-to-day activities (Weller and Budson 2018). Age is the major risk factor for AD and the risk of developing AD increases 2 times for every 5 years for a person above 65 years of age (Querfurth and LaFerla 2010). Pathologically, the presence of neurofibrillary tangles (NFTs) consisting of aggregated tau protein and cerebral plaques containing β - amyloid ($A\beta$) peptides, leading to oxidative damage and inflammation, are the important hallmarks in the diagnosis of AD (Braak and Braak 1991; Querfurth and LaFerla 2010). There is a need for developing newer drugs since the drugs available currently treat the patient only symptomatically (Weller and Budson 2018).

Tau is a heat stable and a tubulin binding protein, which is essential for the assembly of microtubules. It has multiple phosphorylation sites for kinases, such as cAMP-dependent protein kinases and type I casein kinase, to act upon. Phosphorylation significantly affects the ability of tau to bind to tubulin, which is greatest when tau protein is not

✉ Sahabudeen Sheik Mohideen
sahabuds@srmist.edu.in

Vignesh Sundararajan
vs2829@srmist.edu.in

G. Devanand Venkatasubbu
devanang@srmist.edu.in

¹ Department of Biotechnology, School of Bioengineering, SRM Institute of Science and Technology, Kattankulathur, Tamil Nadu 603203, India

² Department of Physics and Nanotechnology, SRM Institute of Science and Technology, Kattankulathur, Tamil Nadu 603203, India

phosphorylated (Jameson et al. 1980; Lindwall and Cole 1984; Pierre and Nunez 1983; Weingarten et al. 1975). In pathological states such as AD, there is an excess production of phosphorylated tau which does not bind to tubulin and gets accumulated intracellularly. The amyloid cascade hypothesis first proposed by Hardy et al. has since become the focal point of AD research, especially in familial forms of AD (Hardy and Higgins 1992). This hypothesis postulates that increased deposition of A β peptide, found in extracellular plaques, is the first and major trigger for the subsequent damages that occur in AD. Amyloid precursor protein (APP) is the precursor from which A β peptide is produced. This initial event leads to the formation of NFTs, which are characterised by the presence of phosphorylated tau protein (p-tau), subsequently leading to neuronal cell death, vascular damage and dementia (Hardy and Allsop 1991; Hardy and Selkoe 2002; Hardy and Higgins 1992). While the presence of A β peptide results in structural and morphological changes to dendritic spines, the death of neurons proceeds only when both A β and tau protein are present. Furthermore, the presence of hyperphosphorylated tau, even in the absence of NFTs, can elicit neuronal toxicity (Bakota and Brandt 2016).

Cerium oxide nanoparticles (nCeO₂) have gained widespread interest among researchers recently as a potential therapeutic compound since it can act as an antioxidant by mimicking the activities of catalase and superoxide dismutase (SOD), and as a scavenger of free radicals (Dowding et al. 2012; Korsvik et al. 2007; Pirmohamed et al. 2010; Szymanski et al. 2015). nCeO₂ exerts both antioxidant and pro-oxidant activities. It elicits beneficial effects, mainly by its ability to decrease oxidative stress, by acting as an antioxidant. It also elicits detrimental effects by causing inflammation, endocrine imbalance, genotoxicity and oxidative stress (Adebayo et al. 2018; Alaraby et al. 2015b; Ali et al. 2015; Azari et al. 2019; Eriksson et al. 2018; Nemmar et al. 2017; Schwotzer et al. 2017; Tisi et al. 2019; Vafaei-Pour et al. 2018).

nCeO₂ have been recently explored as a potential therapeutic to treat AD in vitro and in vivo, mainly using the A β model. It was reported that nCeO₂ acted as a beneficial compound by scavenging free radicals, reducing the aggregation of A β , favouring the survival of neurons, and improving mitochondrial functions (Cimini et al. 2012; Dowding et al. 2014; Kwon et al. 2016; Zhao et al. 2016). However, there are no studies to date that have investigated the efficacy of nCeO₂ in a tau model of AD.

Drosophila is a commonly used in vivo model for studying the toxicity elicited by various nanoparticles and the mode of administration is mainly via the oral route (Alaraby et al. 2015a; Dan et al. 2019; Mishra et al. 2017; Sundararajan et al. 2019). It has a short life cycle of 10–12 days (Ong et al. 2015) and comparison with the human genome

revealed an approximately 60% sequence homology in genetic makeup of humans and *Drosophila* (Wangler et al. 2015), thus emphasising its importance as an invaluable and cost-effective model for understanding the complexity of normal as well as pathological mechanisms in humans. Transgenic disease models can also be obtained in *Drosophila* via genetic manipulation by the use of GAL4-UAS system for tissue-specific expression of target gene (Brand and Perrimon 1993).

In this study, nCeO₂ synthesised via the hydroxide-mediated approach were investigated for their ability to ameliorate commonly observed biochemical, genetic and behavioural changes in human tau (htau)-induced AD in *Drosophila*. To the best of the authors' knowledge, no studies have been performed to date that investigate the therapeutic potential of nCeO₂ in a tau model of AD using *Drosophila*. elav-GAL4 and GMR-GAL4 flies were crossed with UAS-htau/TM3 flies to overexpress htau in the neurons and eyes of the F1 progeny (Sheik Mohideen et al. 2015). Such flies expressing the htau protein were administered nCeO₂ orally along with food for one month, at concentrations of 0.1 and 1 mM, to study the biochemical levels of SOD, AChE, the locomotor activity of flies, and mRNA expression of htau. Moreover, autophagy was hypothesised as one of the mechanisms responsible for tau clearance based on previous reports (Krüger et al. 2012; Sheik Mohideen et al. 2015; Wang et al. 2010; Zhang et al. 2017) and therefore, the gene expression of important autophagy markers such as autophagy-related 1 (ATG1), ATG12, and ATG18 was investigated in the current study.

Materials and methods

Materials

Agar–agar type I was bought from HiMedia, Mumbai. The chemicals bought from SRL Chemicals, Mumbai include acetylthiocholine iodide, potassium chloride, 5,5'-dithiobis-2-nitrobenzoic acid (DTNB), nitrobluetetrazolium (NBT), sodium hydroxide, D-glucose, chloroform, bovine serum albumin (BSA), nicotinamide adenine dinucleotide hydride (NADH), glacial acetic acid, phenazonium methosulphate (PMS), and yeast extract powder. Propionic acid was procured from Merck Life Sciences, Mumbai. Orthophosphoric acid was purchased from Thermo Fischer Scientific, Mumbai.

Synthesis of nCeO₂

nCeO₂ were synthesised via the wet chemical method using sodium hydroxide and cerium nitrate hexahydrate as precursors, as previously described (Sundararajan et al. 2019).

Briefly, a pinkish-white precipitate was formed following drop-wise addition of sodium hydroxide (0.3 M) to sodium nitrate hexahydrate (0.1 M), under constant stirring and heating for 2 h. The final yellow-coloured product obtained after centrifugation, ethanol wash and annealing is nCeO₂. Characterisation of the synthesised nCeO₂ was performed using transmission electron microscopy (TEM), Fourier transform infrared (FTIR) spectroscopy, Raman spectroscopy and X-ray diffraction (XRD) studies.

Concentration and duration of nCeO₂ administration

A previous study by Sundararajan et al. has reported the toxicity elicited by nCeO₂ when administered orally, using 0.05% BSA as the dispersion medium, at concentrations of 0.1 and 1 mM to Oregon-K flies. It was observed that one month administration of both concentrations of nCeO₂ were not toxic to adult male flies (Sundararajan et al. 2019). Therefore, in the current study, the treatment period for nCeO₂ administration to transgenic flies was fixed to one month for performing biochemical and gene expression studies. 0.05% BSA was used as a vehicle control for elav-GAL4 and untreated AD flies.

Generation of Alzheimer's disease model (GMR; htau and elav; htau)

A *Drosophila* model of AD expressing wild-type human tau (htau) in the eyes was obtained by crossing 15 virgin females of GMR-GAL4 with 5 males of UAS-htau/TM3 in control and nCeO₂-containing food (0.1 and 1 mM). The new born male flies exhibiting the phenotype of shrunken eyes with long hair (referred to as GMR; htau) were collected and maintained in nCeO₂-containing food for one month at concentrations of 0.1 and 1 mM, for performing the gene expression studies. The food was changed every week. Similarly, an AD model with a pan-neuronal expression of htau was obtained by crossing 15 virgin females of elav-GAL4 with 5 males of UAS-htau/TM3 in control and treatment food. The new born male flies with the phenotype of normal eyes and long hair (referred to as elav; htau) were maintained in nCeO₂-containing food for one month at concentrations of 0.1 and 1 mM, for performing biochemical and climbing assays. elav-GAL4 flies were used as control to compare the data from transgenic flies. The flies were reared at 25 ± 1 °C and on a 12 h dark–light cycle, with 60% humidity on standard cornmeal diet consisting of corn flour, D-glucose, sugar, agar–agar type 1, and yeast extract powder. Anti-fungal agents such as propionic acid and orthophosphoric acid were added to the cornmeal diet at 55 °C after autoclaving to prevent the growth of fungus.

GMR-GAL4 flies used in the current study were established by Takahashi et al., using P element-mediated germ

line transformation. They have a normal eye morphology and carry pGMR-GAL4 on the X chromosome (Takahashi et al. 1999). UAS- htau/TM3 flies previously established by Mohideen et al. were used in the current study (Sheik Mohideen et al. 2015). elav^{C155} (elav-GAL4, BL#458) flies were procured from *Drosophila* Genetic Resource Center, Kyoto Institute of Technology, Japan. GMR-GAL4 and UAS- htau/TM3 were gifted by Drs. Fumiko Hirose (University of Hyogo, Japan) and Leo Tsuda (National Centre for Geriatrics and Gerontology, Japan).

SOD activity in elav; htau fly heads

The activity of the antioxidant enzyme SOD in control and elav; htau fly heads dissected from flies from control and treatment food (five replicates per treatment group, 20 heads/group) was measured colorimetrically, based on its ability to inhibit the formation of chromogen (Sundararajan et al. 2019). Briefly, 0.15 mL of the supernatant obtained by homogenising 20 elav; htau heads in 0.1 M sodium phosphate buffer was added to 0.2 mL of milliQ water, 1 mL of 0.052 M sodium pyrophosphate buffer (pH 8), 0.3 mL of NBT, and 0.1 mL of 186 µM PMS. Upon adding 0.2 mL of 780 µM NADH to the above mixture, the reaction proceeds with the formation of a purple colour. Acetic acid was used to stop the reaction and absorbance was measured at 560 nm to express the results in the form of SOD units/per/min/mg of protein, by considering 50% inhibition of chromogen production at room temperature as one unit of enzyme activity.

AChE activity in elav; htau heads

Ellman's method was used for the biochemical estimation of the enzyme AChE in control and elav; htau fly heads (five replicates per treatment group, 20 heads/group) dissected from flies from control and treatment food after one month exposure (Sundararajan et al. 2019). Briefly, 0.1 mL of the supernatant obtained by homogenising 20 fly heads in 0.1 M sodium phosphate buffer was added to 100 µL of 10 mM DTNB, 650 µL of 0.1 M sodium phosphate buffer (pH 7.4) and 10 µL of 0.075 M acetylthiocholine iodide. The absorbance of the chromogen was read every minute (for a total of 10 min) at 412 nm to express the results in the form of AChE activity/min/mg of protein.

Climbing assay

To perform the climbing assay, 25 control and elav; htau flies born in control and nCeO₂-containing food were maintained in control and treatment food for one month (five replicates per treatment group). The flies were exposed to new treatment food every week. Following the treatment period, 20 flies/per treatment group were transferred into

empty vials that had a marking at 3 cm from the bottom of the vial. A video was recorded once the flies began to climb after being brought down by gentle tapping, and the ratio of flies that moved beyond the 3 cm mark to total number flies depicted the final results in the form of percentage (Sundararajan et al. 2019).

Quantitative Real-Time PCR (qRT-PCR)

Fifteen GMR; htau flies from the control (untreated GMR; htau) and nCeO₂ treatment groups were anaesthetised via CO₂ exposure and their heads were dissected (three replicates per treatment group). RNA was extracted from the heads via the Trizol Method (Invitrogen). The purity and quantity of the isolated RNA were estimated via Nanodrop (Thermo Scientific), and cDNA was synthesised using 500 ng of RNA (iScript cDNA synthesis kit, Bio-Rad). The mRNA expression of htau, ATG1, ATG12, and ATG18 genes was analysed via qRT-PCR, using a 20- μ L reaction mixture consisting of 2 \times TB Green® Premix Ex Taq™ II (Takara) and gene-specific primers on a QuantStudio 5 Real-Time PCR system (Applied Biosystems). The relative mRNA expression was calculated using the comparative C_T ($\Delta\Delta C_T$) method and RP49 was used as the housekeeping gene. All the samples were run in duplicates. cDNA amplification for all the genes was performed at 95 °C for 5 min, 40 cycles of 95 °C for 15 s and 60 °C for 35 s. The melt curve stage had the following conditions: 95 °C, 60 °C, and 95 °C for 15 s, 1 min, 1 s, respectively. While manually designed primers were used for ATG1, ATG12 and ATG18 (Primer3 Plus online software), the primers for htau and RP49 were used based on a previous publication (Ando et al. 2016). Table 1 lists the primers used in this study.

Statistical analysis

All the values in the graphs are represented in the form of mean \pm SEM. One-way ANOVA followed by Bonferroni's multiple comparison post-test was used to assess the significance of treatment groups with control and untreated AD flies in GraphPad Prism 5.0. $P < 0.05$ was set as the criterion for a denoting a statistically significant value.

Results and discussion

Characterisation of nCeO₂

The FTIR spectrum of the nanoparticle was performed to characterise the different functional groups present within it (Fig. 1a). The FTIR spectrum confirmed the formation of cerium oxide. The spectrum showed peaks at 3430 and 1620 cm⁻¹ which correspond to the hydroxyl groups. The band at 500 cm⁻¹ denoted the Ce–O stretching vibration. The peak around 1450 cm⁻¹ was formed as a result of the bending vibration of C–H stretching. Moreover, N–O stretching resulted in the formation of a peak at 1382 cm⁻¹. Figure 1b shows the XRD image of cerium oxide nanoparticles. The XRD image confirmed the formation of pure cerium oxide. The peaks at $2\theta = 29.3^\circ, 33.3^\circ, 47.45^\circ, 57.5^\circ, 59.2^\circ, 77.2^\circ$ and 78.4° corresponded to (111), (200), (220), (311), (222), (331) and (420) planes, respectively. The absence of any other phase confirmed the purity of the sample. The peak broadening confirmed that the formed samples were in the nanometer range. The XRD confirmed the cubic fluorite structure of nCeO₂. The shape and size of the synthesised particles were elucidated via TEM imaging. The particles were spherically shaped and ranged in size from 20 to 25 nm (Fig. 1c). Raman spectroscopy was performed to investigate if there were any defects in the crystal structure of the synthesised nCeO₂ (Fig. 1d). The Raman spectrum showed a single Raman band at 461 cm⁻¹, which confirmed the formation of cubic fluorite-structured cerium oxide. It had an F_{2g} symmetry. It also displayed a sharp and a symmetric peak. This corresponded to Ce–O–Ce symmetric vibration. The observed single peak at 461 cm⁻¹ was due to first-order scattering.

Biochemical levels of SOD in elav; htau heads

The biochemical levels of SOD in the homogenate of heads of elav; htau transgenic flies were estimated to determine the balance of oxidant/antioxidant and oxidative stress in AD. The SOD units/min/mg of protein were 17.6, 12.8, 14.7, and 17.7 for control, untreated elav; htau, 0.1, and 1 mM treatment groups, respectively. Compared to control, there was a statistically significant decrease in SOD activity of the

Table 1 List of primers used in the gene expression studies

Gene	Forward	Reverse
Htau	CAAGACAGACCACGGGGCGG	CTGCTTGGCCAGGGAGGCAG
RP49	GCTAAGCTGTGCGACAAATG	GTTTCGATCCGTAACCGATGT
ATG1	TCACGAAGAAGGGACAACCTGA	ATGACCAGGCTGACGCAATC
ATG12	GCAGAGACACCAGAATCCCAG	GTGGCGTTCAGAAGGATACAAA
ATG18	GTGTTTCGTCAACTTCAACCAGA	TGTCCAGGGTCGAGTCCAC

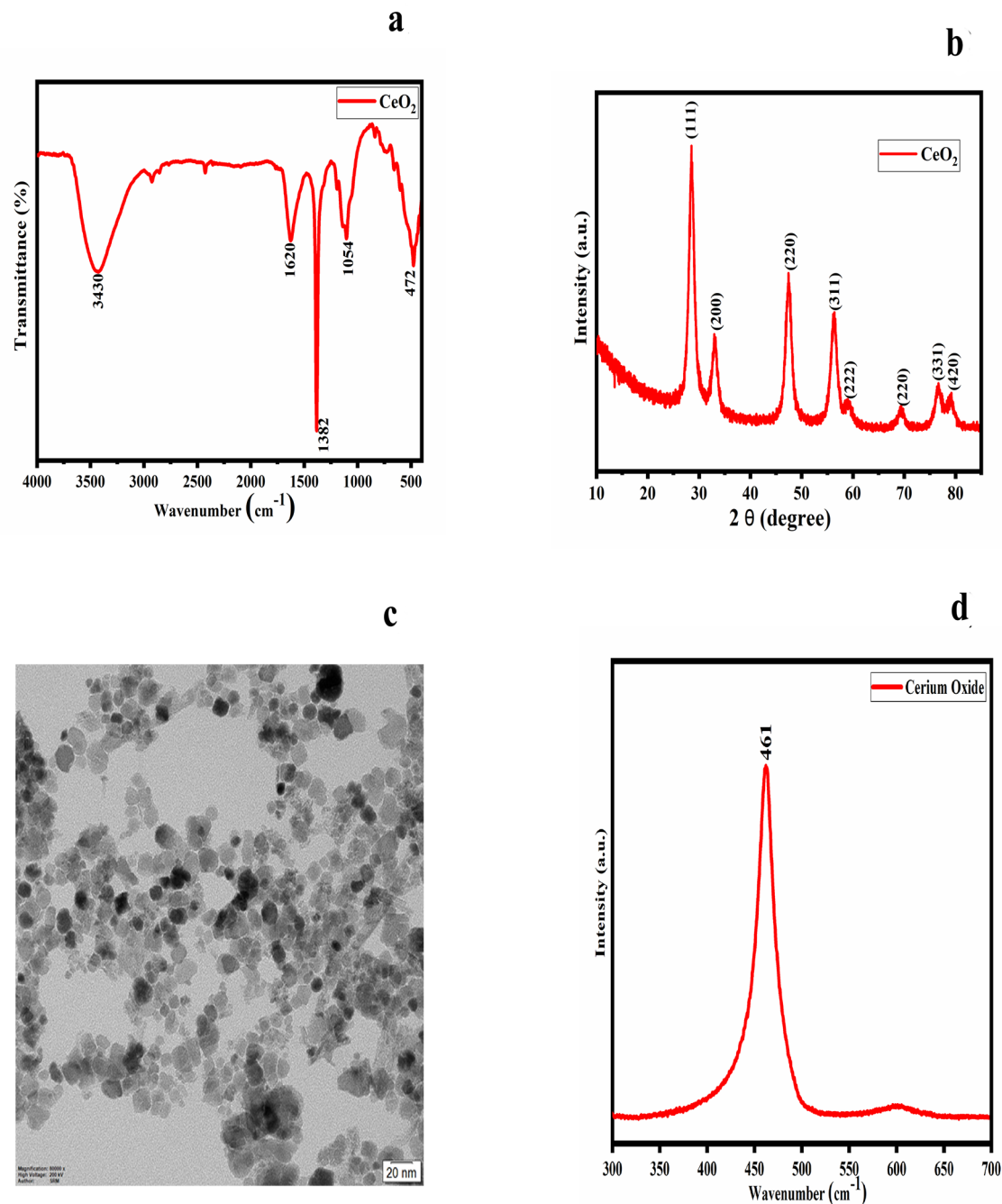


Fig. 1 Characterisation of nCeO₂. **a** FTIR spectrum; **b** XRD analysis; **c** TEM imaging, and **d** Raman spectrum. In the FTIR spectrum, the peaks at 500, 1382 and 1450 cm⁻¹ denoted the Ce–O stretching, N–O stretching, and C–H stretching vibrations, respectively. The peaks at 3430 and 1620 cm⁻¹ were formed due to the presence of the hydroxyl groups. In XRD analysis, the presence of peaks corresponding to (111), (200), (220), (311), (222), (331) and (420) planes

confirmed the polycrystalline nature and purity of the sample. TEM imaging revealed that the particles were spherically shaped, with an average size between 20 and 25 nm. The Raman spectrum showed a single Raman band at 461 cm⁻¹, which confirmed the formation of cubic fluorite-structured cerium oxide. nCeO₂: cerium oxide nanoparticles; FTIR: Fourier transform infrared; XRD: X-ray diffraction; TEM: transmission electron microscopy

untreated elav; htau group ($P < 0.05$) and the 1 mM treatment group helped in restoring the enzyme activity similar to that of control flies. Comparison between the untreated elav; htau group and nCeO₂ treatment groups revealed a

statistically significant increase in SOD activity ($P < 0.05$) for the 1 mM treatment group (Fig. 2). The increase in SOD activity following treatment with nCeO₂ was most likely due to the SOD-mimicking activity of nCeO₂ (Baldim et al.

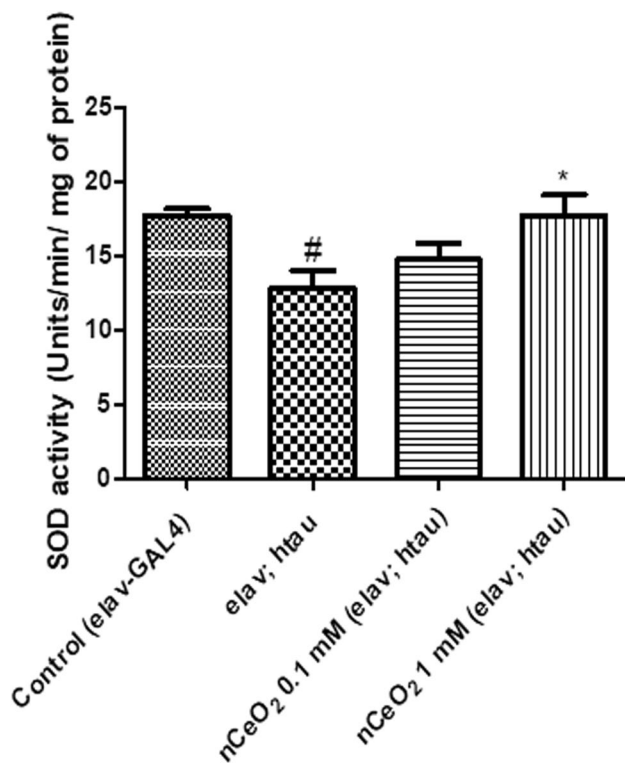


Fig. 2 SOD activity in the heads of elav; htau flies exposed to nCeO₂, dispersed in 0.05% BSA, for one month along with food. 0.05% BSA was used as a vehicle control for elav-GAL4 (control) and untreated elav; htau flies. Values represented are mean ± SEM. Five replicates per treatment group and 20 fly heads per treatment group, ^{*}*P* < 0.05 vs. elav; htau, [#]*P* < 0.05 vs. control. SOD superoxide dismutase, nCeO₂ cerium oxide nanoparticles, BSA bovine serum albumin

2018). SOD is an antioxidant enzyme that acts on the free radical superoxide anion to convert it to hydrogen peroxide. It has three major isoforms, SOD1, SOD2 and SOD3, which differ in the localisation within the cell (Fukai and Ushio-Fukai 2011). Oxidative stress plays a major role in the brain damage of patients with AD and antioxidant enzymes such as SOD are significantly reduced in the blood and brain of patients suffering from AD (Casado et al. 2008; Ihara et al. 1997; Marcus et al. 1998). Compounds that can increase the activity of antioxidant enzymes therefore have the ability to aid in the recovery of neuronal cells from oxidative damage (Alamro et al. 2020). The restoration of SOD activity to normal levels following treatment with nCeO₂ at a concentration of 1 mM suggests that it might confer beneficial effects to neuronal cells undergoing oxidative stress and apoptosis.

Biochemical levels of AChE in elav; htau heads

The biochemical levels of AChE, an important neurotransmitter, were also estimated in the homogenate of heads of elav; htau transgenic flies after dietary exposure to nCeO₂ for one month (Fig. 3). The AChE units/min/mg

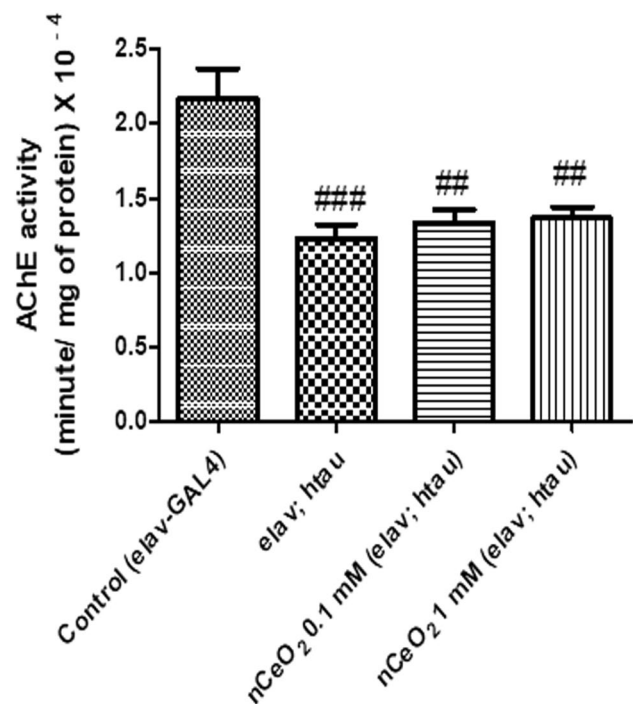


Fig. 3 AChE activity in the heads of elav; htau flies exposed to nCeO₂, dispersed in 0.05% BSA, for one month along with food. 0.05% BSA was used as a vehicle control for elav-GAL4 (control) and untreated elav; htau flies. Values represented are mean ± SEM. Five replicates per treatment group and 20 fly heads per treatment group, ^{###}*P* < 0.001 vs. control, ^{##}*P* < 0.01 vs. control. AChE acetylcholinesterase, nCeO₂ cerium oxide nanoparticles, BSA bovine serum albumin

of protein × 10⁻⁴ were 2.16, 1.27, 1.33 and 1.36 for control, untreated elav; htau, 0.1, and 1 mM treatment groups, respectively. Compared to control, there was a statistically significant decrease in AChE activity of untreated elav; htau flies (*P* < 0.001). Comparison of the enzyme activity of the control group with nCeO₂ treatment groups revealed a significant decrease for 0.1 and 1 mM concentrations (*P* < 0.01). However, there was no significant difference in the enzyme activity when compared with the untreated elav; htau group. This indicates that nCeO₂ did not possess AChE inhibitory activity. Inhibition of AChE activity is one of the therapeutic targets used in patients with AD to provide symptomatic relief due to the presence of cholinergic deficits. Some of the commonly prescribed AChE inhibitors to patients suffering from AD include galantamine, rivastigmine, and donepezil (Mehta et al. 2012). Depletion of neurons specialising in cholinergic functions in regions of the brain associated with learning and memory is a common finding in patients suffering from AD and AChE inhibitors compensate for this by increasing the concentration of acetylcholine in synaptic cleft (Saify and Sultana 2014). Pathogenic forms of tau protein bind to synaptic vesicles to reduce

the rate of neurotransmission in neurons (Zhou et al. 2017). AChE inhibitors, by preventing the breakdown of acetylcholine, upregulate cholinergic neurotransmission and improve deficits associated with memory and learning (Kandimalla and Reddy 2017).

Climbing assay

The climbing assay was performed to evaluate the extent of recovery from tau-induced climbing deficits following one month dietary exposure to nCeO₂. Pan-neuronal expression of htau in *Drosophila* leads to a number of phenotypical, pathological, and behavioural changes such as shortened lifespan, climbing defects, learning and memory deficits and brain vacuolisation (Gistelinck et al. 2012; Mershin et al. 2004; Wittmann et al. 2001). 77.67% of flies from the control group, 48.5% of flies from the untreated elav; htau group, 64.2% of flies from the 0.1 mM nCeO₂ treatment group, and 35.7% of flies from the 1 mM nCeO₂ treatment group climbed beyond the mark of 3 cm. There was a significant decrease in the climbing activity of flies from the untreated elav; htau group ($P < 0.05$) and the 1 mM treatment group ($P < 0.001$), when compared with control flies. Treatment with nCeO₂ at both concentrations for one month failed to elicit any significant improvements in the climbing activity, when compared with the untreated elav; htau group (Fig. 4). The levels of sarkosyl insoluble tau in neurons upon htau expression directly affects the climbing activity of elav;htau flies and improvements in climbing defects is related to the decrease in the amount of insoluble tau (Sheik Mohideen et al. 2015). Therefore, the lack of significant improvements in climbing defects in nCeO₂-treated elav; htau flies could be due to absence of changes in the amount of sarkosyl insoluble tau. The decrease in climbing activity following the administration of nCeO₂ at a concentration of 1 mM could also be due to the detrimental effects elicited by nCeO₂.

Gene expression of htau and ATG genes in GMR; htau fly heads

The effect of one month dietary administration of nCeO₂ to transgenic GMR; htau flies on the mRNA expression of htau and ATG genes was analysed using qRT-PCR. Administration of nCeO₂ along with food resulted in a concentration-dependent decrease in htau gene expression and increase in ATG1 gene expression ($P < 0.05$ for 0.1 mM and $P < 0.01$ for 1 mM), when compared with control flies. No significant effect was seen on the ATG12 gene expression for both concentrations of nCeO₂. However, ATG18 gene expression was significantly increased in the 0.1 mM treatment group ($P < 0.01$), as well as in the 1 mM treatment group ($P < 0.05$), when compared

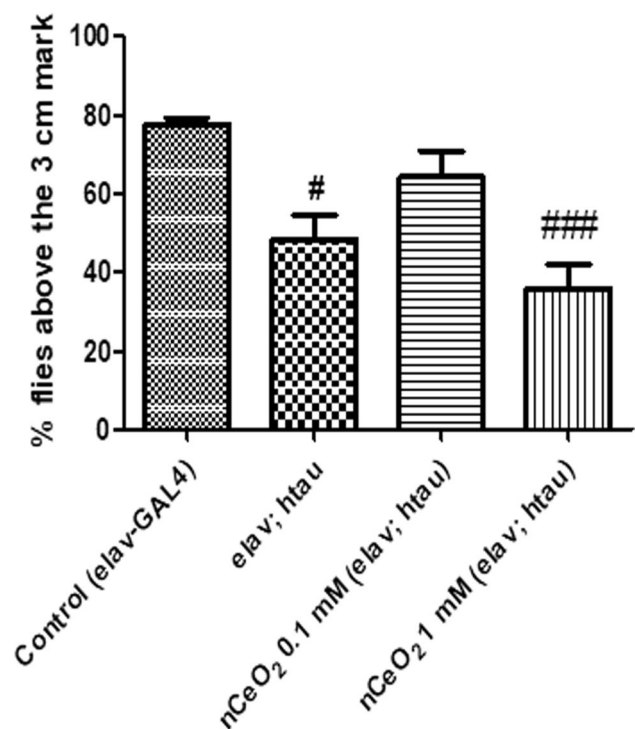


Fig. 4 Climbing activity of elav; htau flies exposed to nCeO₂, dispersed in 0.05% BSA, for one month along with food. 0.05% BSA was used as a vehicle control for elav-GAL4 (control) and untreated elav; htau flies. Values represented are mean \pm SEM. Five replicates per treatment group and 20 elav; htau flies per treatment group, # $P < 0.05$ vs. control, ### $P < 0.001$ vs. control. nCeO₂ cerium oxide nanoparticles, BSA bovine serum albumin

with control flies (Fig. 5). Based on the results obtained, it can be suggested that htau mRNA reduction is most likely due to induction of the autophagy pathway. Cells often use autophagy to maintain homeostasis in normal as well as diseased states, wherein the fusion of autophagosomes to lysosomes results in the removal of unwanted substrates such as protein aggregates, cellular organelles and pathogens (Di Mecco et al. 2020; Shpilka et al. 2012). Dysfunction of autophagy is one of the important causes of neuronal death in AD, due to impaired clearance of misfolded and aggregated proteins such as tau. Therefore, in AD, compounds capable of activating the autophagy pathway to clear aggregated proteins have therapeutic potential (Di Mecco et al. 2020; Li et al. 2017). ATG1 is the part of the ATG1 complex and is important for autophagosome formation (Davies et al. 2015; Yamamoto and Ohsumi 2014). ATG12 along with ATG5 and ATG16L1 is known as the autophagy elongation complex, and is one of the two essential conjugation systems involved in the elongation of the autophagosome (Fahmy and Labonté 2017; Goldsmith et al. 2014). ATG18 is required in the formation of autophagosomes and is also shed by mature autophagosomes before its fusion with

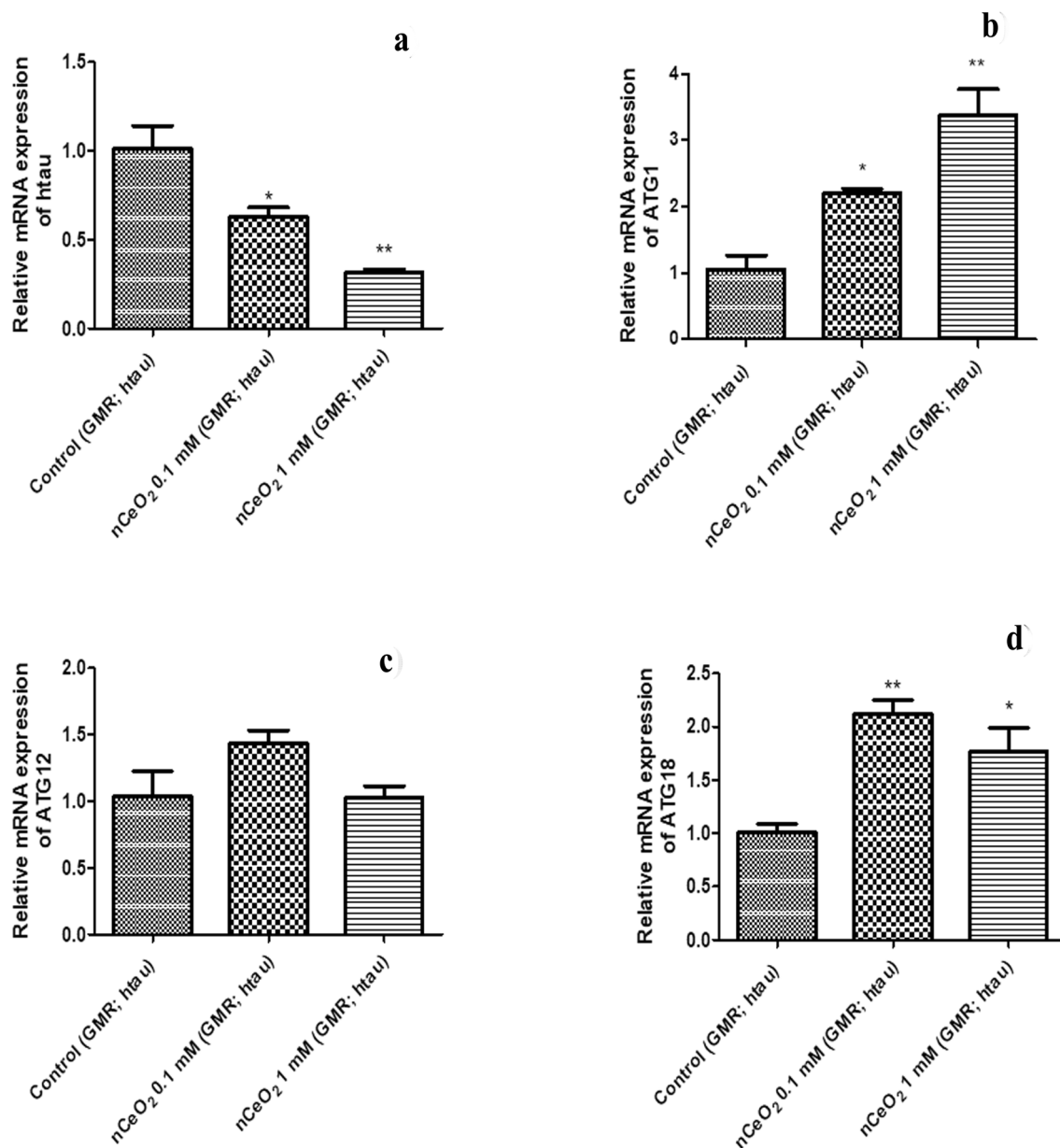


Fig. 5 The relative mRNA expression of htau and ATG genes in the heads of GMR; htau flies exposed to nCeO₂, dispersed in 0.05% BSA, for one month along with food. 0.05% BSA was used as a vehicle control for untreated GMR; htau (control) flies. The gene expression was normalised using RP49 and presented compared to control

values. Data represent the mean \pm SEM. Three replicates per treatment group and 15 fly heads per treatment group, * $P < 0.05$ vs. control, ** $P < 0.01$ vs. control. *htau* human tau, *ATG* autophagy related, *nCeO₂* cerium oxide nanoparticles, *BSA* bovine serum albumin

lysosomes. The level of ATG18 can thus be used to correlate the rate at which autophagosome formation takes place (Domínguez-Martín et al. 2017). nCeO₂ could be a potential therapeutic compound for the treatment of AD if the effects seen at the transcriptional level could also be mimicked at the translational level. Therefore, future

studies could be performed to study the protein expression of htau, p-tau and autophagy markers.

Conclusion

The current study was performed to investigate the therapeutic potential of nCeO₂ in htau-induced *Drosophila* models of AD. nCeO₂ were dispersed in 0.05% BSA and administered to transgenic *Drosophila* as part of their diet for one month, at concentrations of 0.1 and 1 mM. In the GMR; htau model of AD, dietary administration of nCeO₂ at both concentrations activated the autophagy pathway and helped in significantly reducing the levels of htau at the transcriptional level. In the elav; htau model of AD, nCeO₂ at a concentration of 1 mM also helped in restoring the levels of SOD, an antioxidant enzyme commonly depleted in the brain of patients with AD, similar to that of control flies. However, it failed to elicit any neuroprotective effect and it also affected the climbing activity of elav; htau flies at a concentration of 1 mM. The results of this preliminary study suggest that nCeO₂ have limited beneficial effects in htau models of AD and they may also exert detrimental effects at higher concentrations. Therefore, in future studies, the safety and neuroprotective effect of nCeO₂ in htau models of AD should be investigated in detail.

Acknowledgements Dr Sahabudeen acknowledges the Department of Science and Technology (DST) –Science and Engineering Research Board (FILE NO. ECR/2016/000490) for providing financial assistance. The authors acknowledge HRTEM, XRD and Raman facilities at SRM Institute of Science and Technology set up with support from MNRE (Project No. 31/03/2014-15/PVSE-R&D), Government of India. The authors acknowledge the SRM-DBT Platform for Advanced Life Sciences for providing the facility for performing Real-Time PCR experiments. The authors also thank Mr. V.P. Narayanan Nampoothiri for technical assistance.

Declarations

Conflict of interest The authors declare that there is no conflict of interest in the publication.

References

- Adebayo OA, Akinloye O, Adaramoye OA (2018) Cerium oxide nanoparticle elicits oxidative stress, endocrine imbalance and lowers sperm characteristics in testes of balb/c mice. *Andrologia*. <https://doi.org/10.1111/and.12920>
- Alamro AA, Alsulami EA, Almutlaq M, Alghamedi A, Alokail M, Haq SH (2020) Therapeutic potential of vitamin d and curcumin in an in vitro model of alzheimer disease. *J Cent Nerv Syst Dis* 12:1179573520924311. <https://doi.org/10.1177/1179573520924311>
- Alaraby M, Annangi B, Hernández A, Creus A, Marcos R (2015a) A comprehensive study of the harmful effects of ZnO nanoparticles using *Drosophila melanogaster* as an in vivo model. *J Hazard Mater* 296:166–174. <https://doi.org/10.1016/j.jhazmat.2015.04.053>

- Alaraby M et al (2015b) Antioxidant and antigenotoxic properties of CeO₂ NPs and cerium sulphate: Studies with *Drosophila melanogaster* as a promising in vivo model. *Nanotoxicology* 9:749–759. <https://doi.org/10.3109/17435390.2014.976284>
- Ali D, Alarifi S, Alkahtani S, AlKahtane AA, Almalik A (2015) Cerium oxide nanoparticles induce oxidative stress and genotoxicity in human skin melanoma cells. *Cell Biochem Biophys* 71:1643–1651. <https://doi.org/10.1007/s12013-014-0386-6>
- Ando K, Oka M, Ohtake Y, Hayashishita M, Shimizu S, Hisanaga S, Iijima KM (2016) Tau phosphorylation at Alzheimer's disease-related Ser356 contributes to tau stabilization when PAR-1/MARK activity is elevated. *Biochem Biophys Res Commun* 478:929–934. <https://doi.org/10.1016/j.bbrc.2016.08.053>
- Azari A, Shokrzadeh M, Zamani E, Amani N, Shaki F (2019) Cerium oxide nanoparticles protects against acrylamide induced toxicity in HepG2 cells through modulation of oxidative stress. *Drug Chem Toxicol* 42:54–59. <https://doi.org/10.1080/01480545.2018.1477793>
- Bakota L, Brandt R (2016) Tau biology and tau-directed therapies for Alzheimer's disease. *Drugs* 76:301–313. <https://doi.org/10.1007/s40265-015-0529-0>
- Baldirim V, Bedioui F, Mignet N, Margail I, Berret JF (2018) The enzyme-like catalytic activity of cerium oxide nanoparticles and its dependency on Ce³⁺ surface area concentration. *Nanoscale* 10:6971–6980. <https://doi.org/10.1039/C8NR00325D>
- Braak H, Braak E (1991) Demonstration of amyloid deposits and neurofibrillary changes in whole brain sections. *Brain Pathol* 1:213–216. <https://doi.org/10.1111/j.1750-3639.1991.tb00661.x>
- Brand AH, Perrimon N (1993) Targeted gene expression as a means of altering cell fates and generating dominant phenotypes. *Development* 118:401–415
- Casado A, Encarnación López-Fernández M, Concepción Casado M, de La Torre R (2008) Lipid peroxidation and antioxidant enzyme activities in vascular and Alzheimer dementias. *Neurochem Res* 33:450–458. <https://doi.org/10.1007/s11064-007-9453-3>
- Cimini A et al (2012) Antibody-conjugated PEGylated cerium oxide nanoparticles for specific targeting of Aβ aggregates modulate neuronal survival pathways. *Acta Biomater* 8:2056–2067. <https://doi.org/10.1016/j.actbio.2012.01.035>
- Dan P et al (2019) Evaluation of hydroxyapatite nanoparticles - induced in vivo toxicity in *Drosophila melanogaster*. *Appl Surf Sci* 484:568–577. <https://doi.org/10.1016/j.apsusc.2019.04.120>
- Davies CW, Stjepanovic G, Hurley JH (2015) How the Atg1 complex assembles to initiate autophagy. *Autophagy* 11:185–186. <https://doi.org/10.4161/15548627.2014.984281>
- Di Meco A, Curtis ME, Lauretti E, Praticò D (2020) Autophagy dysfunction in Alzheimer's disease: mechanistic insights and new therapeutic opportunities. *Biol Psychiatry* 87:797–807. <https://doi.org/10.1016/j.biopsych.2019.05.008>
- Domínguez-Martín E, Cardenal-Muñoz E, King JS, Soldati T, Coria R, Escalante R (2017) Methods to monitor and quantify autophagy in the social amoeba *dictyostelium discoideum*. *Cells* 6:18. <https://doi.org/10.3390/cells6030018>
- Dowding JM, Dosani T, Kumar A, Seal S, Self WT (2012) Cerium oxide nanoparticles scavenge nitric oxide radical (·NO). *Chem Commun (Camb)* 48:4896–4898. <https://doi.org/10.1039/c2cc30485f>
- Dowding JM et al (2014) Cerium oxide nanoparticles protect against Aβ-induced mitochondrial fragmentation and neuronal cell death. *Cell Death Differ* 21:1622–1632. <https://doi.org/10.1038/cdd.2014.72>
- Eriksson P et al (2018) Cerium oxide nanoparticles with antioxidant capabilities and gadolinium integration for MRI contrast enhancement. *Sci Rep* 8:6999. <https://doi.org/10.1038/s41598-018-25390-z>

- Fahmy AM, Labonté P (2017) The autophagy elongation complex (ATG5-12/16L1) positively regulates HCV replication and is required for wild-type membranous web formation. *Sci Rep* 7:40351. <https://doi.org/10.1038/srep40351>
- Fukai T, Ushio-Fukai M (2011) Superoxide dismutases: role in redox signaling, vascular function, and diseases. *Antioxid Redox Sign* 15:1583–1606. <https://doi.org/10.1089/ars.2011.3999>
- Gistelink M, Lambert JC, Callaerts P, Dermaut B, Dourlen P (2012) *Drosophila* models of tauopathies: what have we learned? *Int J Alzheimers Dis* 2012:970980. <https://doi.org/10.1155/2012/970980>
- Goldsmith J, Levine B, Debnath J (2014) Chapter two—Autophagy and cancer metabolism. In: Galluzzi L, Kroemer G (eds) *Methods in enzymology*, vol 542. Academic Press, Cambridge, pp 25–57. <https://doi.org/10.1016/B978-0-12-416618-9.00002-9>
- Hardy J, Allsop D (1991) Amyloid deposition as the central event in the aetiology of Alzheimer's disease. *Trends Pharmacol Sci* 12:383–388. [https://doi.org/10.1016/0165-6147\(91\)90609-V](https://doi.org/10.1016/0165-6147(91)90609-V)
- Hardy J, Selkoe DJ (2002) The amyloid hypothesis of Alzheimer's disease: progress and problems on the road to therapeutics. *Science (New York, NY)* 297:353. <https://doi.org/10.1126/science.1072994>
- Hardy JA, Higgins GA (1992) Alzheimer's disease: the amyloid cascade hypothesis. *Science (New York, NY)* 256:184–185. <https://doi.org/10.1126/science.1566067>
- Ihara Y et al (1997) Free radicals and superoxide dismutase in blood of patients with Alzheimer's disease and vascular dementia. *J Neurol Sci* 153:76–81. [https://doi.org/10.1016/S0022-510X\(97\)00172-X](https://doi.org/10.1016/S0022-510X(97)00172-X)
- Jameson L, Frey T, Zeeberg B, Dalldorf F, Caplow M (1980) Inhibition of microtubule assembly by phosphorylation of microtubule-associated proteins. *Biochemistry* 19:2472–2479. <https://doi.org/10.1021/bi00552a027>
- Kandimalla R, Reddy PH (2017) Therapeutics of neurotransmitters in Alzheimer's disease. *J Alzheimers Dis* 57:1049–1069. <https://doi.org/10.3233/JAD-161118>
- Korsvik C, Patil S, Seal S, Self WT (2007) Superoxide dismutase mimetic properties exhibited by vacancy engineered ceria nanoparticles. *Chem Commun (Camb)*. <https://doi.org/10.1039/b615134e>
- Krüger U, Wang Y, Kumar S, Mandelkow E-M (2012) Autophagic degradation of tau in primary neurons and its enhancement by trehalose. *Neurobiol Aging* 33:2291–2305. <https://doi.org/10.1016/j.neurobiolaging.2011.11.009>
- Kwon HJ et al (2016) Mitochondria-Targeting Ceria Nanoparticles as Antioxidants for Alzheimer's Disease. *ACS Nano* 10:2860–2870. <https://doi.org/10.1021/acsnano.5b08045>
- Li Q, Liu Y, Sun M (2017) Autophagy and Alzheimer's disease. *Cell Mol Neurobiol* 37:377–388. <https://doi.org/10.1007/s10571-016-0386-8>
- Lindwall G, Cole RD (1984) Phosphorylation affects the ability of tau protein to promote microtubule assembly. *J Biol Chem* 259:5301–5305
- Marcus DL, Thomas C, Rodriguez C, Simberkoff K, Tsai JS, Strafaci JA, Freedman ML (1998) Increased peroxidation and reduced antioxidant enzyme activity in Alzheimer's disease. *Exp Neurol* 150:40–44. <https://doi.org/10.1006/exnr.1997.6750>
- Mehta M, Adem A, Sabbagh M (2012) New acetylcholinesterase inhibitors for Alzheimer's disease. *Int J Alzheimers Dis* 2012:728983–728983. <https://doi.org/10.1155/2012/728983>
- Mershin A, Pavlopoulos E, Fitch O, Braden BC, Nanopoulos DV, Skoulakis EM (2004) Learning and memory deficits upon TAU accumulation in *Drosophila* mushroom body neurons. *Learn Mem* 11:277–287. <https://doi.org/10.1101/lm.70804>
- Mishra M, Sabat D, Ekka B, Sahu S, P U, Dash P, (2017) Oral intake of zirconia nanoparticle alters neuronal development and behaviour of *Drosophila melanogaster*. *J Nanopart Res* 19:282. <https://doi.org/10.1007/s11051-017-3971-y>
- Nemmar A, Yuvaraju P, Beegam S, Fahim MA, Ali BH (2017) Cerium oxide nanoparticles in lung acutely induce oxidative stress, inflammation, and DNA damage in various organs of mice. *Oxid Med Cell Longev* 2017:9639035. <https://doi.org/10.1155/2017/9639035>
- Ong C, Yung L-YL, Cai Y, Bay B-H, Baeg G-H (2015) *Drosophila melanogaster* as a model organism to study nanotoxicity. *Nanotoxicology* 9:396–403. <https://doi.org/10.3109/17435390.2014.940405>
- Pierre M, Nunez J (1983) Multisite phosphorylation of tau proteins from rat brain. *Biochem Biophys Res Commun* 115:212–219. [https://doi.org/10.1016/0006-291x\(83\)90991-9](https://doi.org/10.1016/0006-291x(83)90991-9)
- Pirmohamed T et al (2010) Nanoceria exhibit redox state-dependent catalase mimetic activity. *Chem Commun (Camb)* 46:2736–2738. <https://doi.org/10.1039/b922024k>
- Querfurth HW, LaFerla FM (2010) Alzheimer's disease. *N Engl J Med* 362:329–344. <https://doi.org/10.1056/NEJMra0909142>
- Saify ZS, Sultana N (2014) Chapter 7—Role of acetylcholinesterase inhibitors and Alzheimer disease. In: Attaur R, Choudhary MI (eds) *Drug design and discovery in Alzheimer's disease*. Elsevier, Amsterdam, pp 387–425. <https://doi.org/10.1016/B978-0-12-803959-5.50007-6>
- Schwotzer D, Ernst H, Schaudien D, Kock H, Pohlmann G, Dasenbrock C, Creutzenberg O (2017) Effects from a 90-day inhalation toxicity study with cerium oxide and barium sulfate nanoparticles in rats. *Part Fibre Toxicol* 14:23. <https://doi.org/10.1186/s12989-017-0204-6>
- Sheik Mohideen S, Yamasaki Y, Omata Y, Tsuda L, Yoshiike Y (2015) Nontoxic singlet oxygen generator as a therapeutic candidate for treating tauopathies. *Sci Rep* 5:10821. <https://doi.org/10.1038/srep10821>
- Shpilka T, Mizushima N, Elazar Z (2012) Ubiquitin-like proteins and autophagy at a glance. *J Cell Sci* 125:2343. <https://doi.org/10.1242/jcs.093757>
- Sundararajan V, Dan P, Kumar A, Venkatasubbu GD, Ichihara S, Ichihara G, Sheik Mohideen S (2019) *Drosophila melanogaster* as an in vivo model to study the potential toxicity of cerium oxide nanoparticles. *Appl Surf Sci* 490:70–80. <https://doi.org/10.1016/j.apsusc.2019.06.017>
- Szymanski CJ et al (2015) Shifts in oxidation states of cerium oxide nanoparticles detected inside intact hydrated cells and organelles. *Biomaterials* 62:147–154. <https://doi.org/10.1016/j.biomaterials.2015.05.042>
- Takahashi Y, Hirose F, Matsukage A, Yamaguchi M (1999) Identification of three conserved regions in the DREF transcription factors from *Drosophila melanogaster* and *Drosophila virilis*. *Nucleic Acids Res* 27:510–516. <https://doi.org/10.1093/nar/27.2.510>
- Tisi A, Passacantando M, Lozzi L, Riccitelli S, Bisti S, Maccarone R (2019) Retinal long term neuroprotection by Cerium Oxide nanoparticles after an acute damage induced by high intensity light exposure. *Exp Eye Res* 182:30–38. <https://doi.org/10.1016/j.exer.2019.03.003>
- Vafaei-Pour Z, Shokrzadeh M, Jahani M, Shaki F (2018) Embryoprotective effects of cerium oxide nanoparticles against gestational diabetes in mice. *Iran J Pharm Res* 17:964–975
- Wang Y, Krüger U, Mandelkow EM (2010) Generation of tau aggregates and clearance by autophagy in an inducible cell model of tauopathy. *Neurodegener Dis* 7:103–107. <https://doi.org/10.1159/000285516>
- Wangler MF, Yamamoto S, Bellen HJ (2015) Fruit flies in biomedical research. *Genetics* 199:639–653. <https://doi.org/10.1534/genetics.114.171785>

- Weingarten MD, Lockwood AH, Hwo SY, Kirschner MW (1975) A protein factor essential for microtubule assembly. *Proc Natl Acad Sci USA* 72:1858–1862. <https://doi.org/10.1073/pnas.72.5.1858>
- Weller J, Budson A (2018) Current understanding of Alzheimer's disease diagnosis and treatment. *F1000Res* 7:F1000 Faculty Rev-1161. doi: <https://doi.org/10.12688/f1000research.14506.1>
- Wittmann CW, Wszolek MF, Shulman JM, Salvaterra PM, Lewis J, Hutton M, Feany MB (2001) Tauopathy in *Drosophila*: neurodegeneration without neurofibrillary tangles. *Science* (New York, NY) 293:711–714. <https://doi.org/10.1126/science.1062382>
- Yamamoto H, Ohsumi Y (2014) Chapter 4—The molecular mechanisms underlying autophagosome formation in yeast. In: Hayat MA (ed) *Autophagy: cancer, other pathologies, inflammation, immunity, infection, and aging*. Academic Press, Amsterdam, pp 67–77. <https://doi.org/10.1016/B978-0-12-405529-2.00004-4>
- Zhang Z-H et al (2017) Selenomethionine mitigates cognitive decline by targeting both tau hyperphosphorylation and autophagic clearance in an alzheimer's disease mouse model. *J Neurosci* 37:2449–2462. <https://doi.org/10.1523/jneurosci.3229-16.2017>
- Zhao Y, Xu Q, Xu W, Wang D, Tan J, Zhu C, Tan X (2016) Probing the molecular mechanism of cerium oxide nanoparticles in protecting against the neuronal cytotoxicity of A β 1–42 with copper ions. *Metalomics* 8:644–647. <https://doi.org/10.1039/c5mt00242g>
- Zhou L et al (2017) Tau association with synaptic vesicles causes presynaptic dysfunction. *Nat Commun* 8:15295. <https://doi.org/10.1038/ncomms15295>